Applied Food Research 4 (2024) 100545

Contents lists available at ScienceDirect

Applied Food Research

journal homepage: www.elsevier.com/locate/afres

Conventional and ultrasound-assisted extractions of protein from sacha inchi (*Plukenetia volubilis*) and their impact on the physicochemical and structural characteristics

Rosana Chirinos [a,*], Romina Scharff-Salinas [a], Jamerccy Rodriguez-Diaz [a], Andrés Figueroa-Merma [a], Ana Aguilar-Galvez [a], Fanny Guzmán [b], Ingrid Contardo [c,d], Romina Pedreschi [e,f], David Campos [a,*]

[a] Instituto de Biotecnología (IBT), Universidad Nacional Agraria La Molina (UNALM). Av. La Molina s/n, Lima 12056, Peru
[b] Núcleo de Biotecnología Curauma (NBC), Pontificia Universidad Católica de Valparaíso (PUCV), Valparaíso, Av. Universidad 330, Curauma, Valparaíso, Chile
[c] Biopolymer Research & Engineering Laboratory (BiopREL), School of Nutrition and Dietetics, Faculty of Medicine, Universidad de los Andes, Chile. Monseñor Álvaro del Portillo 12.455, Las Condes, Chile
[d] Centro de Investigación e Innovación Biomédica (CiiB), Universidad de los Andes, Chile. Monseñor Álvaro del Portillo 12.455, Las Condes, Santiago 7620086, Chile
[e] Escuela de Agronomía, Pontificia Universidad Católica de Valparaíso (PUCV), Calle San Francisco s/n, La Palma, Quillota, Chile
[f] Millennium Institute Center for Genome Regulation (CRG), Santiago, Chile

ARTICLE INFO

Keywords:
Protein
Plukenetia volubilis
Oil press-cake
Ultrasound-assisted extraction
Conventional extraction
Secondary structures

ABSTRACT

This study aimed to evaluate the recovery of proteins from sacha inchi (SI) cake, using two methods: conventional extraction by alkaline solubilization (SIC, pH 10.5, time 60 min, solvent/sample ratio 40/1) and ultrasound-assisted method (SIUS), the latter undergoing optimization using response surface methodology. The protein powder concentrate obtained by SIUS reached a protein content of ~ 72 % (dry weight, DW), under the optimized conditions of amplitude: 48 %, solvent/sample ratio: 50 mL/g and time: 19 min at pH 10.5, compared to that obtained using the conventional method with ~77 % (DW). The physicochemical and structural characteristics differentiate both protein concentrates, the SIUS protein presented a slightly darker color, a narrower size particle distribution, a higher specific surface area, and a manifest denaturation as evidenced by the thermal analysis, compared to that obtained for SIC protein. The structural modifications of the proteins were evaluated by FTIR and circular dichroism (CD) spectroscopy, FTIR showed that the total proteins in SIUS had a decrease in β-sheet and an increase in β-turn configuration, whereas the soluble proteins evaluated by CD presented a marked decrease in α-helix and an increase in random coil and β-sheet configurations. The results contribute to offering information for future applications for both protein concentrates from SI cake in the food sector.

1. Introduction

In the current nutritional scenario, there is a need to explore alternative protein sources to meet the growing world demand, in addition to the task of identifying resources with high protein content to replace animal proteins (Sá et al., 2021), which are increasingly less affordable owing to their availability and price. The adoption of plant-based diets is of paramount importance in promoting environmental sustainability, safeguarding human health, and ensuring the welfare of animals (Samad et al., 2024). Currently, society is interested in incorporating a greater amount of vegetable protein into their diet, which could be used for different purposes, such as fat replacers, flavor enhancers, food and beverage stabilizers and nutritional supplements, or as inputs for obtaining protein hydrolysates for special diets or bioactive peptides. The exploration of potential protein sources together with the concept of circular economy leads us to pay special attention to the by-products of the agroindustry, evaluating possible forms for their utilization. In this scenario, the by-products of the oil industry (e.g., main residue is oil-cake) have gained importance especially for those cakes coming from oilseed and legume grains, whose protein content is high.

The Sacha Inchi (SI) is widely distributed along the western and northern edge of the Amazon basin, through Brazil, Bolivia, Peru,

* Corresponding authors.
E-mail addresses: chiri@lamolina.edu.pe (R. Chirinos), dcampos@lamolina.edu.pe (D. Campos).

https://doi.org/10.1016/j.afres.2024.100545
Received 29 July 2024; Received in revised form 24 September 2024; Accepted 7 October 2024
Available online 9 October 2024

Ecuador, Colombia, Venezuela, Suriname, and in the Lesser Antilles (Goyal et al., 2022). SI is a plant native to the San Martin and Loreto regions of the Peruvian Amazon. The SI seed is valued for its high oil content (between 35 and 60 %), with ω−3 and ω−6 fatty acids and proteins (between 25 and 30 %). It also contains bioactive compounds, such as tocopherols, phytosterols and polyphenols (Hameker et al., 1992; Guillén et al., 2003; Chirinos et al., 2013; Rawdkuen et al., 2016; Gutiérrez et al., 2019). Studies have suggested that SI cake obtained after oil extraction has the potential to produce protein concentrates/isolates, protein fractions, functional ingredients or nutraceuticals (e.g. protein hydrolysates or bioactive peptides) (Chirinos et al., 2017; 2020; Cordero-Clavijo et al., 2024; Suwanangul et al., 2021; Torres-Sánchez et al., 2023).

Conventional extraction of proteins from vegetable sources is performed in alkaline media (pH 9.0 - 11.0) to recover the proteins by isoelectric precipitation. New extraction technologies have appeared seeking to replace or assist the conventional method allowing improvements in protein extraction yield, as well as in their techno-functional, nutritional and functional properties, and shorter extraction times. Novel technologies evaluated for protein extraction are microwave-assisted extraction, ultrasound-assisted extraction, pressurized liquid extraction and pulsed electric field, all based on achieving optimal cell disruption (Pojić et al., 2018). The use of ultrasound and microwave technologies stand out as the most convenient from the point of view of economy, processing and energy efficiency. Ultrasound is based on the generation and use of acoustic waves, which when transferred to a liquid medium produce compression and rarefaction effects. This bring about the formation, growth and subsequent collapse of microbubbles, inducing cavitation, which increases the porosity of the matrix by inducing the formation of micro-fissures and channels that increase the permeation of solvent into the matrix (Maroun et al., 2018), impacting the extraction yield of molecules bound to cell wall components and intracellular matrices (Zhang et al., 2011). Ultrasonication is generally used as a pretreatment method in the conventional protein solubilization protocols because it can break the cell matrix to improve the extractability (Tawalbeh et al., 2023). Ultrasonication is also applied to modify the physical, structural, and functional properties of protein-based ingredients, besides simultaneous extraction and modifications (Rahman & Lamsal, 2021).

Most studies that have evaluated SI cake protein extraction have relied on conventional extraction based on alkaline solubilization (Chirinos et al., 2017; Suwanangul et al., 2021; Torres-Sánchez et al., 2023; Sathe et al., 2012; Rawdkuen et al., 2022). Some have evaluated enzyme-assisted extraction (Chirinos et al., 2017; Rawdkuen et al., 2022) and a recent study has employed ultrasound-assisted extraction using 100 % amplitude, for a time of 15 min at pH 9 and 11 (Cordero-Clavijo et al., 2024). Therefore, there is a need to deepen or broaden the studies aimed at evaluating protein extraction processes from SI cake and characterizing them to provide more information on their potential future use. Since SI cake is an important source of proteins, the use of ultrasound could increase yields and/or improve extraction parameters, as well as obtain proteins differentiated in their physicochemical and structural characteristics. These are aspects that have been scarcely explored to date, and studying them could open up new lines of research on SI protein and its potential applications. Thus, the main objectives of the present study were: 1) to optimize the extraction of protein from SI cake by means of ultrasound-assisted extraction, using the response surface methodology (MSR) considering a Box-Behnken design; and 2) to evaluate the influence of the extraction method, ultrasound-assisted and conventional, on the physicochemical and structural characteristics of the proteins.

2. Materials and methods

2.1. Materials and chemicals

The SI cake was purchased from a local company in Lima (Peru). The cake was obtained after extraction of the SI seed oil using an expeller press. SI cake was presented as a flour-like powder (particle size < 500 μm) of a light-yellow color. Total protein, fat and moisture content were determined in the SI cake (using AOAC 920.87, AOAC 2003.05 and AOAC 934.01 methods, respectively). Chemicals, solvents and others required for analysis were purchased from Sigma-Aldrich (St Louis, Mo, USA), J.T. Baker® (Phillipsburg, NJ, USA) and Merck (Darmstadt, Germany).

2.2. Protein extraction

2.2.1. Conventional extraction

Conventional extraction was performed following the methodology proposed by Chirinos et al. (2017) with slight modifications. Briefly, the SI cake was dissolved in distilled water at a 40/1 (v/w) ratio, the pH was brought to 10.5 with 1 N NaOH under agitation at 50 °C for 1 h, extraction was conducted in an orbital shaker (GLF, model 1092, Germany) at 300 rpm. Subsequently, the mixture was centrifuged (Eppendorf, model 5430R, Germany) at 8452 x *g* for 30 min at 4 °C, recovering the supernatant from which soluble protein was determined. The protein present in the supernatant was recovered by isoelectric precipitation at pH 4.8 with 1 N HCl followed by centrifugation at 8452 x *g* for 20 min at 4 °C. The precipitated protein was washed twice with distilled water, each wash consisted of shaking (200 rpm) the protein solution for 5 min followed by centrifugation at 8452 x *g* for 30 min at 4 °C, then the protein solution was brought to pH 7.0 and freeze dried (Labconco, USA). The powdered product obtained was sieved (< 500 μm) to make the particle size uniform, and finally stored until further analysis.

2.2.2. Ultrasound-assisted extraction

Ultrasound-assisted extraction was performed in a Branson Ultrasonics SFX250 equipment (Branson Ultrasonics Corporation, Danbury, USA) with a 20 kHz converter, placed inside an acoustic chamber. The extractions were performed in 50 mL double-walled cylindrical glass vessels coupled to a cooling system to maintain a constant temperature during the operation. The extractions, considering three factors: amplitude (%), liquid/solid ratio (mL/g) and time (min), were subjected to optimization (see experimental design section). In all tests, the SI cake was dispersed in water at pH 10.5 (with 1 N NaOH), 50 ± 2.0 °C, using a ¾" probe, with *on* and *off* times of 5 s each, according to preliminary studies conducted in our laboratory. Once the extractions were finished, the set was centrifuged (8452 x *g* for 30 min at 4 °C), the supernatant was analyzed for soluble protein and the protein extraction yield was calculated. The treatment that extracted the highest amount of protein went on to the protein recovery process as described in the conventional extraction method.

2.3. Experimental design for ultrasound-assisted protein extraction

Ultrasound-assisted SI cake protein extraction was optimized using a Box-Behnken design (used to allow fitting a second-order model) and response surface methodology (RSM) analysis. Thus, after the development of preliminary tests to adjust the range of values of the factors under study, three factors were considered: amplitude (X_1, 30–50 %), solvent-to-sample ratio (X_2, 20–50 mL/g) and time (X_3, 5–20 min), and each factor was coded at three levels (−1, 0 and +1). A total of 17 experimental runs were performed considering 5 central points (Table 1); and each run was performed in triplicate. The response variable was the protein extraction yield (%). The model (second-order polynomial) proposed among the variables evaluated and the response corresponded to the following equation:

Table 1
Box–Behnken design and experimental results for ultrasound-assisted protein extraction and protein yield responses.

Runs	Ultrasound-assisted				
	Amplitude (%) (X_1)	Ratio (Solvent/ sample, mL/g) (X_2)	Time (min) (X_3)	Protein yield (%)	
				Experimental *	Predicted
1	30 (−1)	20 (−1)	12.5 (0)	32.25 ± 0.09	33.03
2	40 (0)	35 (0)	12.5 (0)	27.92 ± 0.87	29.15
3	50 (+1)	35 (0)	5 (−1)	25.84 ± 1.26	25.61
4	40 (0)	20 (−1)	20 (+1)	37.13 ± 0.10	36.11
5	30 (−1)	50 (+1)	12.5 (0)	31.71 ± 1.73	30.86
6	40 (0)	50 (+1)	20 (+1)	41.21 ± 1.27	41.82
7	40 (0)	35 (0)	12.5 (0)	29.92 ± 1.99	29.15
8	30 (−1)	35 (0)	5 (−1)	19.98 ± 1.63	19.81
9	50 (+1)	50 (+1)	12.5 (0)	43.06 ± 0.67	42.28
10	40 (0)	20 (−1)	5 (−1)	31.55 ± 1.96	30.94
11	40 (0)	35 (0)	12.5 (0)	30.01 ± 2.57	29.15
12	40 (0)	50 (+1)	5 (−1)	28.12 ± 0.68	29.14
13	40 (0)	35 (0)	12.5 (0)	28.93 ± 1.97	29.15
14	30 (−1)	35 (0)	20 (+1)	27.02 ± 2.29	27.25
15	50 (+1)	20 (−1)	12.5 (0)	35.35 ± 2.67	36.20
16	40 (0)	35 (0)	12.5 (0)	28.99 ± 1.89	29.15
17	50 (+1)	35 (0)	20 (+1)	35.86 ± 1.61	36.03

* n = three repetitions ± SD.

$$Y = \alpha_0 + \sum_{i=1}^{n} \alpha_i A + \sum_{i=1}^{n} \alpha_{ii} A_i^2 + \sum_{i=1}^{n} \sum_{i=1}^{n} \alpha_{ij} A_i A_j \quad (1)$$

Where: Y is the response predicted, α_0 is the value of the adjusted response to the central point of the design, αi, αii and αij are the linear coefficient, quadratic coefficient and the intercept, respectively, *Ai, Aj* are the factors, and n is the number of measured variables ($n = 3$).

The optimum protein extraction conditions for each method consisted in determining the maximum protein extraction yield using a combination of different variables. The model obtained was validated by extracting the SI cake protein under optimal conditions, and then comparing the experimental values with the predicted values. Also, three-dimensional surface response plots were generated by varying two variables within the experimental range and holding the others constant at the central points (0). The experimental designs and statistical analyses were performed with Statgraphics Centurion 19-X64 (StatPoint Technologies, Inc., Warrenton, VA, USA).

2.4. Analytical methods

2.4.1. Moisture, dry matter, oil, total protein and soluble protein

Moisture was determined by AOAC (2007) 934.01 based on gravimetric determination of mass loss in an oven until constant mass was achieved, and the results were expressed as percentage. Dry mass was determined by subtracting the value of 100 from the moisture value. Fat content was determined by the Soxhlet method, subjecting the sample to extraction with petroleum ether according to AOAC 2003.05 (AOAC, 2007). Crude protein was determined by the Kjeldahl method - AOAC 920.87 (AOAC, 2007), and a value of 5.7 was used as the nitrogen conversion factor (Sathe et al., 2012). The values of fat and protein content were expressed as percentage. Soluble protein was determined by spectrophotometry at 650 nm following the methodology proposed by Lowry et al. (1951). The amount of soluble protein was estimated from a standard curve of bovine serum albumin (BSA) in the concentration range of 0.5 - 3.0 mg/mL. The results were expressed in mg or g of BSA/mL.

2.4.2. Protein extraction yield

For the optimization tests, the protein extraction yield was determined using the following equation

$$\text{Protein extraction yield}(\%) = \frac{\text{Soluble protein (g/mL) in extract} * \text{extract volume (mL)}}{\text{Total protein(g) of SI cake sample}} * 100 \quad (2)$$

2.4.3. Color

The color of the protein concentrates was determined by the CIELAB method using a Minolta colorimeter (model R-400/410, Osaka, Japan) (Sharma et al., 2023). Prior to the measurements, the colorimeter was calibrated using a white tile. In color measurement, the illuminant C and a 2° standard observer were used. The measurements were performed in triplicate, determining the average values of the characteristics L^* (indicates white to black), a^* (redness to greenness) and b^* (yellowness to blueness). Based on the previous results, the hue angle (h^*) and chroma (C*) values were determined. In addition, a photographic record of the samples was taken.

2.4.4. Particle size analysis

The mean particle size and particle size distribution were determined in triplicate by using a laser diffraction particle size analyzer Mastersizer 3000E (Malvern Instruments Ltd., UK) coupled to a liquid-phase dispersion system (*Hydro* EV) (Jambrak et al., 2014). The samples were dispersed in recirculating ethanol. Diameters referring to 10, 50 and 90 % of the accumulated distribution (D_{10}, D_{50} and D_{90}, respectively) were calculated in μm units and polydispersity was calculated with the span index, according the following equation:

$$Span = \frac{(D_{90} - D_{10})}{D_{50}} \quad (3)$$

Additionally, the specific surface area (m^2/kg) was calculated.

2.4.5. Differential scanning calorimetry (DSC)

Thermal denaturation of SI protein concentrates was evaluated by DSC analysis by using a Perkin Elmer differential scanning calorimeter Pyris 6. The determination was performed following the methodology proposed by Betalleluz-Pallardel et al. (2017), with slight modifications. Briefly, the protein was dissolved in distilled water (20 %, w/v) and the resulting solution was subsequently homogenized and allowed to stand for 1 h. Approximately 60 μL of sample was weighed into an aluminum pan and then hermetically sealed. The pan was heated from 30 to 110 °C at a heating rate of 5 °C/min. An empty pan was used as a reference. For each run, a thermogram was obtained, from which the temperature at which denaturation started (T_{onset}, °C), the denaturation peak temperature (T_d, °C) and enthalpy (Δh, J/g) were determined. The measurements were performed in triplicate.

2.4.6. Secondary structure by fourier transform infrared (FTIR) spectroscopy

Fourier transform infrared (FTIR) spectra were recorded for protein samples (in powder) using a Nicolet IS10 spectrophotometer (Thermo Fisher Scientific, USA) equipped with an attenuated total reflectance (ATR) accessory, according to the method proposed by Shrestha et al. (2023) with slight adaptations. The averaged spectra were obtained over a wavenumber range of 4000–400 cm^{-1} with 32 scans acquired at a spectral resolution of 4 cm^{-1}. All measurements were performed in triplicate. The spectra obtained were processed using OMNIC 9 software, including baseline correction and normalization of the relative absorbance. Protein secondary structures were determined as the percentages of α-helix, β-sheet, β-turn and random coil configurations, using the software OrigingPro 2019b (OriginLab Corporation, Northampton, MA, USA).

2.4.7. Secondary structure by circular dichroism spectroscopy analysis

Circular dichroism (CD) spectra for protein samples were obtained with a Jasco J-815 CD Spectrometer coupled to a Peltier Jasco CDF-426

S/15 temperature controller (Jasco Corp., Tokyo, Japan). Proteins were dissolved at approximately 1 mg/mL in 2 mM phosphate buffer saline (PBS) and then filtered through a 45 μm syringe filter. The measurements were obtained in the ultraviolet range between 190 and 250 nm. A quartz cell with 0.1 cm path length and 1 nm bandwidth was used with signal averaging over 2 s/nm interval. Each spectrum was measured three times in continuous scanning mode at 25 °C. The data analysis was done using Spectra Manager Software version 2.0. CD data were expressed in terms of ellipticity (deg.cm^2/dmol). Finally, CD spectra were deconvoluted to obtain secondary structure of proteins.

2.5. Statistical analysis

Results were expressed as the average of three replicates ± standard deviation. Statistical analyses were performed with Statgraphics Centurion 19-X64 (StatPoint Technologies, Inc., Warrenton, VA, USA). T - test was carried out to determine significant differences ($p < 0.05$) between the treatments.

3. Results and discussion

3.1. Sacha inchi cake and protein extracted by conventional method

Moisture, fat and protein values of the SI cake presented 4.8, 4.42 and 59.9 %, respectively; which were within the ranges previously reported in the literature (Chirinos et al., 2017; Torres-Sánchez et al., 2023). Cordero-Clavijo et al. (2024) reported a higher protein content (~ 67 %) for a SI cake defatted with n-hexane, under 5 continuous extraction stages, supporting the high protein value obtained. Non-polar solvents are very affine to fats, favoring a high recovery. SI cake was obtained with an expeller press, being the usual way of processing SI seeds. On the other hand, a low-fat content (< 5 %) favors protein extraction, since a high oil content can lead to the formation of oil-protein emulsions and interfere with protein recovery, impacting extraction yields.

Conventional extraction by alkaline solubilization resulted in a liquid extract with a SI protein extraction yield of 53 ± 0.57 %, which was higher than the 29.7 % previously reported (Chirinos et al., 2017) where the extraction was optimized using the alkaline solubilization technique in SI cake. The difference can be attributed to the origin of the SI seed as well as to the conditions under which oil extraction was carried out by expeller pressing (e.g. seed moisture, screw speed, temperature, etc.), resulting in cakes with different characteristics. In contrast, the extraction yield of protein was lower than that obtained by Cordero-Clavijo et al. (2024) (66.3 % at pH 11 and temperature below 45 °C) and by Sathe et al. (2012) (~ 60 % with 0.1 M NaOH and temperature of 25 °C). However, as already mentioned, the cake used by the authors was defatted by solvents, which would cause fewer structural changes to the resulting cake against shear and friction stresses than that caused when subjected to expeller extraction, affecting the extraction of protein. After extraction, the protein was recovered by isoelectric precipitation and the final freeze-dried product (SIC) had a protein content of 77.5 % (dry weight, DW).

3.2. Optimization of protein extraction by ultrasound assistance

The experimental results of the ultrasound-assisted extraction are presented in Table 1. From the combination of the factors that resulted in 17 runs, it was found that the extraction yields were in the range between 19.9 and 43.1 %. From the statistical design, a quadratic model describing the protein extraction yield (Y) as a function of the coded independent variables (X_1, X_2 and X_3) was obtained using the following equation:

$$Y(\%) = 62.4721 + 0.114558X_1 - 2.83482X_2 + 0.296056X_3 + 0.01375X_1X_2 + 0.0305911{X_2}^2 + 0.0166889X_2X_3 - 0.02728{X_3}^2 \quad (4)$$

The quadratic model was evaluated statistically to determine the degree of fit to the experimental data through analysis of variance (Table S1). The results indicated that only the interactions X_1, X_3, and $X_1 \times 2$ were not significant ($p > 0.05$), and a high coefficient of determination was obtained ($R^2 = 98.37$ %) indicating that the model fits the experimental data, and that there is a high degree of correlation between the observed and fitted values (R^2 and R^2 adjusted). Therefore, the model is adequate for describing the data with reliable predictions. Additionally, the model showed no significant lack of fit ($p > 0.05$), indicating that the experimental results agreed well with the model.

The response surfaces are shown in Fig. 1(a–c). The effect of the amplitude on the solvent/sample ratio is shown in Fig. 1a. It is observed that the amplitude presents a linear effect with a slight positive slope, while the solvent/sample ratio shows a convex curvature-type behavior, reaching the highest yields towards the highest values within the evaluated ranges.

Fig. 1b presents the effects between amplitude and time, amplitude again presents a linear effect with a positive slope, while time tends to present a curvature effect reaching high protein recovery yields (between 18 and 20 min) at the highest amplitude evaluated (50 %). Finally, the solvent/sample ratio and time effects are shown in Fig. 1c, where the convex curvature effect of the solvent/sample ratio factor with high yields towards the extremes (20 and 50 mL/g); however, it is at the ~ 50 mL/g ratio and at the longest times (between 18 and 20 min) where the highest protein extraction yield was achieved. According to the generated model, the optimal extraction conditions corresponded to an amplitude of 48.5 %, solvent/sample ratio of 50 mL/g, and time of 19.4 min providing predicted protein recovery levels in the range of 43.9 and 47.0 %. For model validation purposes, three runs were performed considering 48 % amplitude, 50 mL/g ratio, and 19 min time, obtaining an experimental value of 46.1 ± 0.49 %, which is within the generated range of the model.

The protein extraction yield obtained by ultrasound-assisted extraction was lower to that obtained by conventional extraction (46% vs 53 %), highlighting the shorter extraction time (19 min compared with 60 min). A similar trend was found by Cordero-Clavijo et al. (2024) with values of 54.8 and 66.3 % for ultrasound-assisted extraction and conventional extraction, respectively. The results could be affected not only by the quality of the raw material related to the defatting method, but also by the conditions of extraction. Ultrasound is a technique based on the generation of high shear energy and macroturbulence leading to the disintegration of the cell membrane and cell wall. This results in increased transfer of the extraction solvent to the disintegrated cells, thereby improving the extraction yield of molecules bound to cell wall components and intracellular matrices (Zhang et al., 2011). Although cavitation and mechanical effects caused by sonication promote protein dissolution, when it reaches a certain (high) level, aggregation of dissolved protein molecules and their denaturation may also occur (Lian et al., 2021), with ultrasound use time playing an important role (Bhargava et al., 2021). Therefore, the SI proteins extracted under ultrasound conditions may have undergone conformational changes affecting their recovery (e.g. formation of aggregates or chemical changes) which could have had an impact on adequate solubility in the aqueous medium. In addition, because ultrasound is an efficient methodology for cell disruption, other compounds may have been extracted together with the proteins, becoming present in the protein extracts and reducing the percentage of protein in the final product. Concentration studies, applying membrane technology followed by the extraction process assisted using ultrasound are proposed as a subsequent stage, to increase the protein content in the final product. The final freeze-dried product was namely SIUS and presented a protein content of 72.3 % (DW).

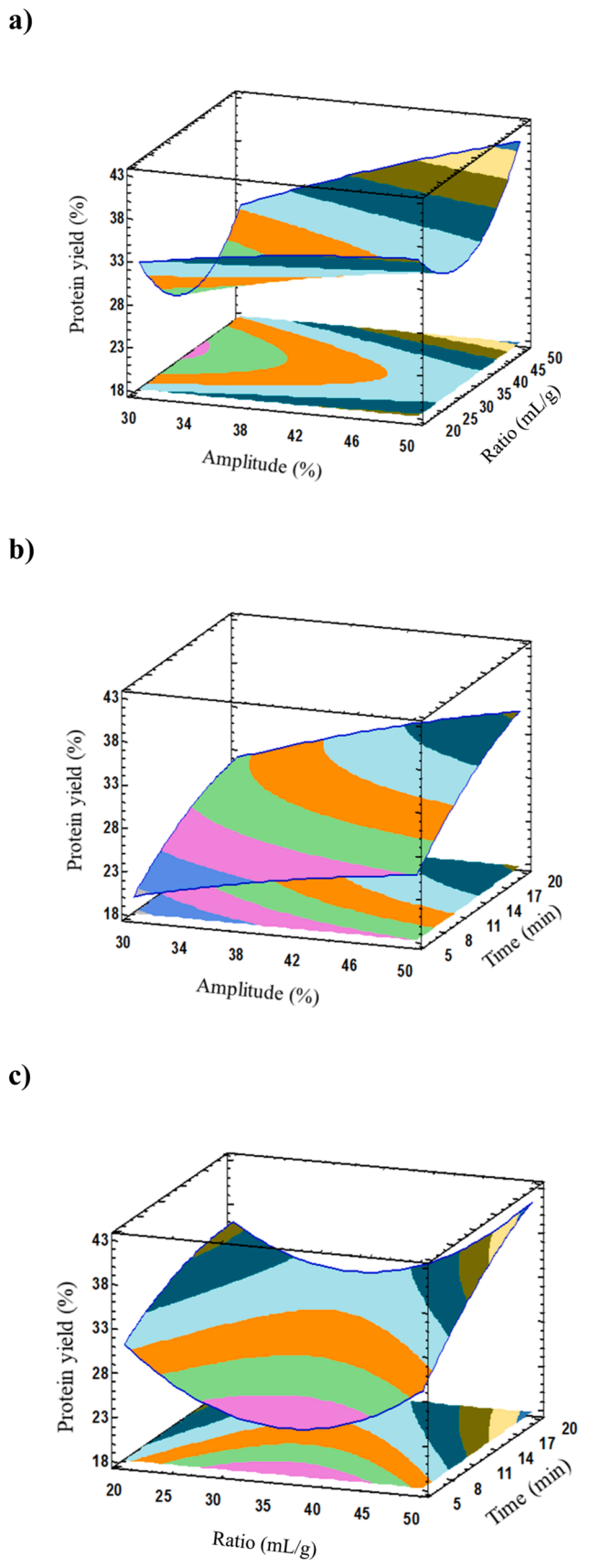

Fig. 1. Response surface for SI cake protein obtained by ultrasound assisted extraction in function of amplitude (%), solvent/sample ratio (mL/g) and time (min). In all cases, the third variable was taken as a mean value.

3.3. Characterization of SI cake proteins obtained by conventional and ultrasound-assisted extractions

3.3.1. Color, particle size and thermal properties

Photographic records of the SI cake proteins recovered by conventional (SIC) and US-assisted (SIUS) extractions are displayed in Fig. 2. The SIUS sample presented a slightly darker color than SIC, which is reflected in the colorimetric values (Table 2) determined through the luminosity (L^*), presenting a darker shift for SIUS. This characteristic could be due to the presence in SIUS of a higher number of other compounds (e.g., phenolic compounds and oxidized compounds, among others) resulting from an efficient cell disruption caused by ultrasound, which may have contributed to the L^* value. The a^*, b^*, C* and h^* values were not significantly different ($p > 0.05$) between the two protein extraction methods. The a^* values, being positive, had a tendency towards red, but of low intensity because they were numerically low, while the positive b^* values had a more marked tendency towards yellow. The C* and h^* characteristics defined as saturation and hue, respectively, support shades tending toward yellow.

The particle size distribution was evaluated using D_{10}, D_{50} and D_{90} values for the SIC and SIUS samples (Table 2). The D_{10} and D_{90} values are a way to represent the smallest and the largest particles present in the product, respectively. Thus, 10 % and 90 % of the total particles of the extracted SI proteins presented sizes (diameters) smaller than the range between 24.9 and 26.4 μm and between 287.7 and 260.0 μm, respectively ($p < 0.05$). Instead, the D_{50} value that represents the average of the median particle size, and the polydispersity index (span) that evaluates the amplitude of size distribution were within 105.7 and 109.0 μm and within 2.4 and 2.1 μm for SIC and SIUS ($p < 0.05$), respectively. The higher D_{50} value for SIUS than for SIC could be due to aggregation between protein particles or aggregation of proteins with other compounds present in the sample resulting from the application of ultrasound but with a lower dispersion between particles. It was also found that specific surface area was higher ($p < 0.05$) in the SIUS than in the SIC sample (146.2 and 141.7 m^2/kg, respectively). In this regard, it has been reported that ultrasound results in the generation of particles with a narrower distribution compared to a process that does not apply it, as well as in generating a higher specific surface area, which coincides with the results here reported. In fact, Jambrak et al. (2014) reported for a whey protein concentrate treated with an ultrasonic probe of 20 kHz, a decrease in particle size that narrowed its distribution and significantly increased the specific free surface. These results were attributed to the ultrasonic vibrations that caused partial denaturation that significantly affected the physical and structural properties of proteins.

The thermograms obtained from SIC and SIUS samples showed only one exothermic peak. The values of T_{onset}, T_d and Δh are presented in Table 2. *Td* represents the thermal stability of the protein and the hydrophobic/hydrophobic interactions of the protein molecules; thus, hydrophobic interactions increase their stability when the temperature increases (high *Td*), whereas electrostatic interactions and hydrogen bonds decrease their stability when the temperature increases (low *Td*) (Betalleluz-Pallardel et al., 2017). Both SIC and SIUS presented similar *Td* values ~ 94.0 °C, being close to soybean protein (96 °C), flaxseed globulins (91.3 °C) and close to the values reported for other plant globulins, in the range from 90 to 105 °C (Li-Chan & Mab, 2002; Pugliese et al., 2017). On the other hand, Δh was higher for SIC (0.146 J/g) than for SIUS (0.114 J/g). Δh *is* associated with molecular changes caused by the unfolding of the protein molecule. This change is a combination of endothermic reactions, such as the breakup of hydrogen bonds, and exothermic reactions, such as protein aggregation and breakup of hydrophobic interactions (Li-Chan & Mab, 2002). Thus, a low Δh of SIUS indicates partial denaturation, which requires less energy to denature. The low Δh of SIUS might be attributed to the application of sonication and alkaline conditions (pH 10.5), which could have enhanced protein solubilization and consequently led to the disruption of its structure. This disruption likely promoted the breaking of protein

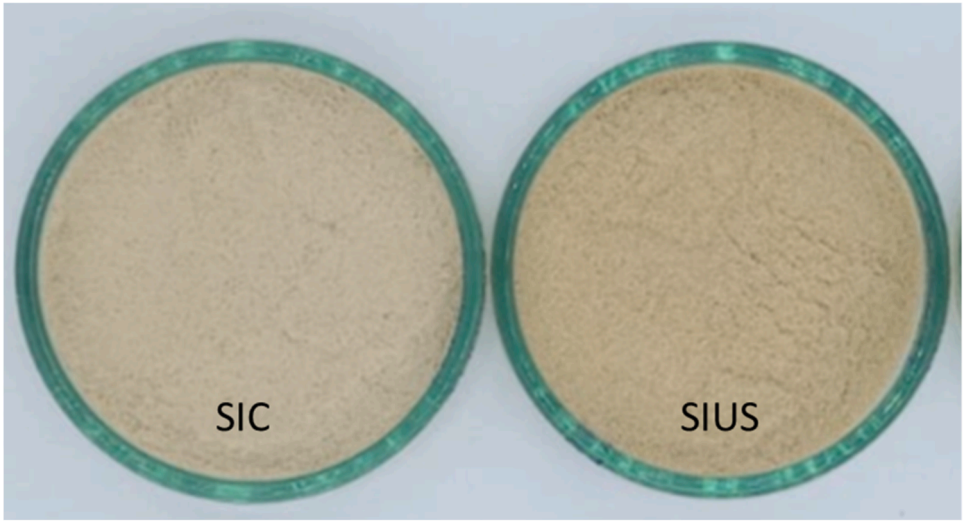

Fig. 2. Photographs of the sachi inchi protein concentrate obtained by conventional extraction (SIC) and by ultrasound-assisted extraction (SIUS).

Table 2
Color, particle size, specific surface area, thermal properties and secondary structures evaluated by FTIR of sacha inchi proteins.

Parameters	Conventional extraction (SIC)	Ultrasound-assisted extraction (SIUS)
	Color CIELAB	
L^*	78.10 ± 0.09^a	74.91±0.04^b
a^*	3.07±0.01^a	3.39±0.05^b
b^*	19.22±0.21^a	19.73±0.17^a
C*	19.47±0.21^{ab}	20.02±0.47^a
h^*	80.94±0.08^a	80.25±0.07^a
	Particle size	
D_{10} (μm)	24.9 ± 0.31^b	26.4 ± 0.12^a
D_{50} (μm)	105.8 ± 1.53^b	109.0 ± 1.00^a
D_{90} (μm)	287.7 ± 6.43^a	260.0 ± 1.00^b
Span (μm)	2.46±0.07^a	2.13±0.03^b
Specific surface area (m^2/kg)	141.7 ± 1.72^b	146.2 ± 0.91^a
	Thermal properties	
T_{onset} (°C)	89.6 ± 0.77^a	90.1 ± 0.07^a
Td (°C)	94.0 ± 0.62^a	93.8 ± 0.05^a
Δh (J/g)	0.146 ± 0.01^a	0.114 ± 0.00^b
	FTIR	
α-helix (%)	28.3 ± 4.6^a	36.7 ± 4.3^a
β-sheet (%)	21.8 ± 3.3^a	12.5 ± 3.5^b
β-turn (%)	16.4 ± 1.0^b	29.5 ± 4.1^a
random coil (%)	33.9 ± 5.3^a	26.3 ± 3.6^a

Different letter between extraction types represents significant differences ($p < 0.05$).

interactions, both inter- and intra-molecular, to a greater extent compared to SIC. Therefore, the formation of new protein structures cannot be ruled out in the process of obtaining SIUS proteins.

3.3.2. Secondary structure evaluated by FTIR and circular dichroism spectroscopy analysis

The secondary structure of the powdered SI protein recovered from conventional and under ultrasound-assisted extractions was evaluated by FTIR and CD analyses. The FTIR spectra in the region from 4000 to 400 cm^{-1} are presented in Fig. 3.

The bands of the FTIR spectrum, amide I (1600–1700 cm^{-1}), and amide II (1500–1600 cm^{-1}) provide information on the presence of proteins in the sample (Arntfield & Murray, 1981). Thus, amide I is associated with the stretching vibrations of the carbonyl group (C=O) of amide and amide II resulting from C-N stretching vibrations coupled with N-H bending vibrations (Ellepola et al., 2005), while amide III

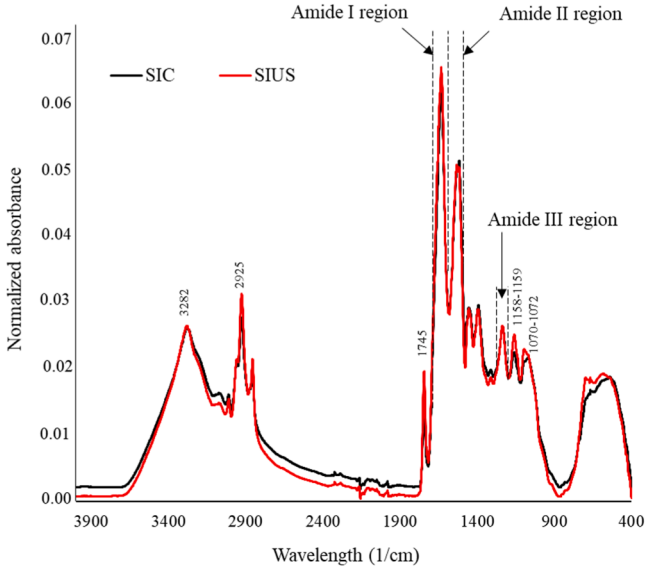

Fig. 3. FTIR spectrum for SI protein obtained by conventional (SIC) and ultrasound assisted (SIUS) extractions.

(1260–1300 cm^{-1}) indicates interactions between proteins and other macromolecules, such as carbohydrates, with C-N stretching and N-H bending vibrations (Wu et al., 2021). SIC and SIUS presented similar spectra, with slight shifts in the intensities and positions of the peaks in amide I (~1635 cm^{-1}), amide II (1532–1533 cm^{-1}), and amide III (1235–1236 cm^{-1}) due to the different treatments followed in the recovery of SI protein. Another characteristic found in both samples, which indicates the presence of proteins, was the high absorption in the bands at ~ 2925 cm^{-1} (amide B) and ~ 3282 cm^{-1} (amide A), which are related to the -OH stretching vibration and C–H antisymmetric shrinkage in the -CH_2 group, respectively (Zhao et al., 2021). In addition, Wu et al. (2021) indicated that the amide A band was the product of stretching vibrations of N-H bond.

Usually, the amide I region is used to estimate the secondary structures of proteins; thus, after applying deconvolution and the second derivative of the spectrum of the amide I region, the participation of different secondary structures (α-helix, β-sheet, β-turn and random coil) in SI proteins was evidenced (Table 2). The participation of secondary structures in decreasing order of importance for SIC protein was:

random coil (33.9 %) > α-helix (28.3 %) > β-sheet (21.8 %) > β-turn (16.4 %), whereas for SIUS was: α-helix (36.7 %) > random coil (26.3 %) > β-turn (29.5 %) > β-sheet (12.5 %), with significant variations ($p < 0.05$) only for β-sheet and β-turn structures. There were fewer β-sheets and more β-turns in SIUS than in SIC. The results for SIC protein differed from those reported by Torres-Sánches et al. (2023) for SI protein extracted at pH 11, which could be due to the differences in the type and participation of the extracted proteins and their concentration (degree of purity) in the samples, which are closely related to the extraction conditions (e.g., temperature) at which the protein was recovered. Albumins (43.7 %), globulins (27.3 %), prolamins (3.0 %), and glutelins (31.9 %) have been found in the SI protein (Sathe et al., 2012).

On the other hand, the structure-level changes found for SIUS partially agree with Ding et al. (2021) who reported increases in α-helix and β-turn and loss of β-sheet configurations in soy protein subjected to an ultrasonic frequency of 35 Hz. Moreover, Zhao et al. (2021) reported that protein extraction from the legume *Dolichos lablab* by ultrasound produced a decrease in random coil structures and an increase in β-turn structures. The decrease, although not significant ($p > 0.05$), of the random coil structure for SIUS would indicate that the proportion of disordered structures was reduced leading to the formation of more stable structures. On the other hand, the presence of other non-protein structures associated with ester functional groups (~ 1745 cm^{-1}) and the probable presence of lipids and polysaccharides (~1159, ~ 1090, 1070 cm^{-1}) was observed in both samples, occurring more intensely in the SIUS samples.

CD was the second analysis employed to determine the participation of the secondary structures of the soluble proteins. These results, together with the spectra obtained (190–250 nm), are presented in Fig. 4. Under this methodology, the α-helix configuration is characterized by three bands: two negative bands at 220–222 nm and 206–209 nm and one positive band at 191–193 nm. The β-sheet configuration is characterized by an intense negative band at ~216 nm and a positive band between 195 and 200 nm. The β-turn configuration is characterized by a weak negative band at 220–230 nm, a more intense negative band at 180–190 nm and a positive band at 200–210 nm. The random coil configuration presents mainly an intense negative band at 195–200 nm. According to the characteristics and after the spectrum deconvolution process, the participation of secondary structures was determined. In the SIC protein the random coil structure stands out (43.4 %), followed by α-helix (20.3 %), β-sheet (20.4 %) and β-turn (15.7 %), while for the SIUS protein the following order was presented: random coil (49.8 %) followed by β-sheet (27.1 %), β-turn (15.6 %) and α-helix (7.3 %). The α-helix configuration was significantly reduced in SIUS ($p < 0.05$) compared to SIC, while random coil configuration was significantly increased. This finding would indicate that the proteins present in SIUS exhibit greater disorganization (higher random coil), a condition likely derived from the α-helix structures (notable reduction) compared to SIC proteins. The differences observed between SIC and SIUS samples are like those found in black bean proteins treated with ultrasound at different ultrasonic powers and times, where a decrease in α-helix and an increase in β-sheet, with no changes in β-turn and random coil configurations (Jiang et al., 2014) and also for a duck liver protein isolate treated with ultrasound (Zou et al., 2017).

On the other hand, when comparing the percentages of participation of the secondary structures found by CD, these are close to those determined by FTIR in the case of SIC protein. However, for SIUS protein there is a significant difference. Shrestha et al. (2023) also observed differences in protein analysis conducted using FTIR and CD, attributing these differences to the protein composition within the samples. Specifically, FTIR analyzes the powdered sample, encompassing both soluble and insoluble proteins, whereas CD focuses on soluble proteins in an aqueous medium, resulting in variations in the outcomes. Consequently, FTIR provides insights into the secondary structure of the total proteins recovered and present in SIC and SIUS, while CD offers data related to the soluble proteins. Therefore, the observed changes in secondary structure are influenced by the type and quantity of protein present in the samples. Additionally, it is possible that non-protein compounds present to a greater extent in SIUS with respect to SIC (27 % with respect to 23 % of non-protein compounds) may have influenced this characteristic.

4. Conclusions

In the present study under the optimized conditions of ultrasound-assisted extraction, a minor amount of protein was extracted (13.2 % less) compared to the conventional method of alkaline solubilization, however, ultrasound reduced the extraction time required by the latter methodology by one-third. Characterization of the obtained SI protein concentrates revealed a protein content of 72.3 % (DW) using ultrasound compared to 77.5 % (DW) with conventional extraction. On the other hand, ultrasound conferred different physical characteristics to the

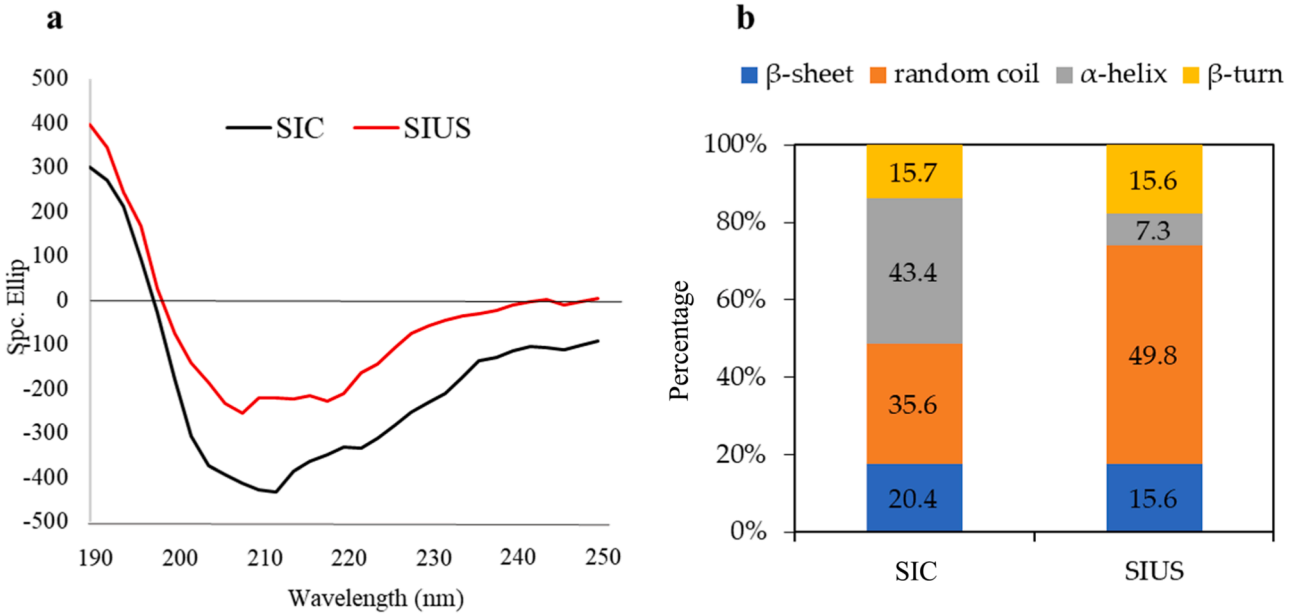

Fig. 4. Circular dichroism spectrum and secondary structures for SI protein obtained by conventional (SIC) and ultrasound assisted (SIUS) extractions.

protein, thus as slightly darker coloration, less particle size dispersion, greater specific surface area, and lower Δh value with respect to the protein recovered in a conventional way, which shows greater denaturation of the protein. At the level of secondary structures, FTIR analysis showed that ultrasound significantly modified the participation of the set of proteins in the protein, such as increasing the β-turn configurations and decreasing the β-sheet configuration, while CD analysis showed changes in the soluble proteins, decreasing the α-helix and increasing the random coil and β-sheet configurations. The findings of this research serve as a starting point for further experimentation related to potential uses of SI protein extracted under ultrasound-assisted technology, such as hydrolyzates, food additives, supplement ingredients, among others.

Funding

This research was supported by the CONCYTEC-PROCIENCIA, Grant N° PE501077970–2022-PROCIENCIA. R. Pedreschi acknowledges ANID - MILENIO - ICN2021_044.

Ethical statement

Studies in humans and animals not applicable

Data availability

Data sharing not applicable.

CRediT authorship contribution statement

Rosana Chirinos: Conceptualization, Methodology, Supervision, Validation, Writing – review & editing. **Romina Scharff-Salinas:** Investigation, Methodology. **Jamerccy Rodriguez-Diaz:** Investigation, Methodology. **Andrés Figueroa-Merma:** Investigation, Methodology. **Ana Aguilar-Galvez:** Methodology, Writing – review & editing. **Fanny Guzmán:** Methodology, Writing – review & editing. **Ingrid Contardo:** Methodology, Validation, Writing – review & editing. **Romina Pedreschi:** Formal analysis, Validation, Writing – original draft, Writing – review & editing. **David Campos:** Methodology, Supervision, Validation, Writing – review & editing.

Declaration of competing interest

The authors declare that they have no known competing financial interests or personal relationships that could have appeared to influence the work reported in this paper.

Supplementary materials

Supplementary material associated with this article can be found, in the online version, at doi:10.1016/j.afres.2024.100545.

References

AOAC. (2007). *Official methods of analysis* (18th ed.). Gaithersburg, Maryland, USA: Association of Official Analytical Chemists.

Arntfield, S. D., & Murray, E. D. (1981). The influence of processing parameters on food protein functionality 1. Differential scanning calorimetry as an indicator of protein denaturation. *Canadian Institute of Food Science and Technology Journal, 14*, 289–294. https://doi.org/10.1016/S0315-5463(81)72929-8

Betalleluz-Pallardel, I., Inga, M., Mera, L., Pedreschi, R., Campos, D., & Chirinos, R. (2017). Optimisation of extraction conditions and thermal properties of protein from the Andean pseudocereal cañihua (*Chenopodium pallidicaule* Aellen). *International Journal of Food Science and Technology, 52*(4), 1026–1034. https://doi.org/10.1111/ijfs.13368

Bhargava, N., Mor, R. S., Kumar, K., & Sharanagat, V. S. (2021). Advances in application of ultrasound in food processing: A review. *Ultrasonic Sonochemistry, 70*, Article 105293. https://doi.org/10.1016/j.ultsonch.2020.105293

Chirinos, R., Pedreschi, R., & Campos, D. (2020). Enzyme-assisted hydrolysates from sacha inchi (*Plukenetia volubilis*) protein with *in vitro* antioxidant and antihypertensive properties. *Journal of Food Processing and Preservation, 44*(12), e14969. https://doi.org/10.1111/jfpp.14969

Chirinos, R., Zuloeta, G., Pedreschi, R., Mignolet, E., Larondelle, Y., & Campos, D. (2013). Sacha inchi (*Plukenetia volubilis*): A seed source of polyunsaturated fatty acids, tocopherols, phytosterols, phenolic compounds and antioxidant capacity. *Food Chemistry, 141*(3), 1732–1739. https://doi.org/10.1016/j.foodchem.2013.04.078

Chirinos, R., Aquino, M., Pedreschi, R., & Campos, D. (2017). Optimized methodology for alkaline and enzyme-assisted extraction of protein from sacha inchi (*Plukenetia volubilis*) kernel cake. *Journal of Food Processing and Preservation, 40*(2), e12412. https://doi.org/10.1111/jfpe.12412

Cordero-Clavijo, L. M., Chuck-Hernández, C., Espinosa-Ramírez, J., Lazo-Vélez, M. A., & Serna-Saldívar, S. O. (2024). Effect of multi factor-assisted extraction (pH, ultrasound, and temperature) of protein from sacha inchi (*Plukenetia volubilis*) and its protein quality and functional characteristics. *Food and Bioproducts Processing, 144*, 156–165. https://doi.org/10.1016/j.fbp.2024.01.014

Ding, Y., Ma, H., Wang, K., Azam, S. M. R., Wang, Y., Zhou, J., et al. (2021). Ultrasound frequency effect on soybean protein: Acoustic field simulation, extraction rate and structure. *LWT Food Science and Techology, 145*, Article 111320. https://doi.org/10.1016/j.lwt.2021.111320

Ellepola, S. W., Choi, S. M., & Ma, C. Y. (2005). Conformational study of globulin from rice (*Oryza sativa*) seeds by Fourier-transform infrared spectroscopy. *International Journal and Biological Macromolecules, 37*(1), 12–20. https://doi.org/10.1016/j.ijbiomac.2005.07.008

Goyal, A., Tanwar, B., Sihag, M. K., & Sharma, V. (2022). Sacha inchi (*Plukenetia volubilis* L.): An emerging source of nutrients, omega-3 fatty acid and phytochemicals. *Food Chemistry, 373*, Article 131459. https://doi.org/10.1016/j.foodchem.2021.131459

Guillén, M. D., Ruiz, A., Cabo, N., Chirinos, R., & Pascual, G. (2003). Characterization of sacha inchi (*Plukenetia volubilis* L.) Oil by FTIR spectroscopy and 1 H NMR. Comparison with linseed oil. *Journal of American Oil Chemists' Society, 80*(8), 755–762. https://doi.org/10.1007/s11746-003-0768-z

Gutiérrez, L. F., Sánchez-Reinoso, Z., & Quiñones-Segura, Y. (2019). Effects of dehulling Sacha inchi (*Plukenetia volubilis* L.) seeds on the physicochemical and sensory properties of oils extracted by means of cold pressing. *Journal of American Oil Chemists' Society, 96*(11), 1187–1195. https://doi.org/10.1002/aocs.12270

Hamaker, B., Valles, C., Culman, R., Hardmeier, R., & Clark, D. G. (1992). Amino acid and fatty acid profile of the Inca peanut. *Cereal Chemistry, 69*(4), 461–463.

Jambrak, A. R., Mason, T. J., Lelas, V., Paniwnyk, L., & Herceg, Z. (2014). Effect of ultrasound treatment on particle size and molecular weight of whey proteins. *Journal of Food Engineering, 121*, 15–23. https://doi.org/10.1016/j.jfoodeng.2013.08.012

Jiang, L., Wang, J., Li, Y., Wang, Z., Liang, J., Wang, R., et al. (2014). Effects of ultrasound on the structure and physical properties of black bean protein isolates. *Food Research International, 62*, 595–601. https://doi.org/10.1016/j.foodres.2014.04.022

Lian, H., Wen, C., Zhang, J., Feng, Y., Duan, Y., Zhou, J., et al. (2021). Effects of simultaneous dual-frequency divergent ultrasound-assisted extraction on the structure, thermal and antioxidant properties of protein from *Chlorella pyrenoidosa*. *Algal Research, 56*, Article 102294. https://doi.org/10.1016/j.algal.2021.102294

Li-Chan, E. C. Y., & Mab, C. Y. (2002). Thermal analysis of flaxseed (*Linum usitatissimum*) proteins by differential scanning calorimetry. *Food Chemistry, 77*, 495–502. https://doi.org/10.1016/S0308-8146(01)00365-X

Lowry, O., Rosebough, N., Lewistarr, A., & Randall, R. (1951). Protein measurement with the Folin phenol reagent. *Journal of Biological Chemistry, 193*, 265–275. https://doi.org/10.1016/S0021-9258(19)52451-6

Maroun, R., Rajha, H., El Darra, N., El Kantar, S., Chacar, S., Debs, E., et al. (2018). Emerging technologies for the extraction of polyphenols from natural sources. In C Galanakis (Ed.), *Polyphenols: Properties, recovery and applications* (pp. 265–293). United Kingdom: Woodhead Publishing, Elsevier. https://doi.org/10.1016/B978-0-12-813572-3.00008-7.

Pojić, M., Mišana, A., & Tiwarib, B. (2018). Eco-innovative technologies for extraction of proteins for human consumption from renewable protein sources of plant origin. *Trends in Food Science Technology, 75*, 93–104. https://doi.org/10.1016/j.tifs.2018.03.010

Pugliese, A., Cabassi, G., Chiavaro, E., Paciulli, M., Carini, E., & Mucchetti, G. (2017). Physical characterization of whole and skim dried milk powders. *Journal of Food Science and Technology, 54*(11), 3433–3442. https://doi.org/10.1007/s13197-017-2795-1

Rahman, M. M., & Lamsal, B. P. (2021). Ultrasound-assisted extraction and modification of plant-based proteins: Impact on physicochemical, functional, and nutritional properties. *Comprehensive Reviews in Food Science and Food Safety, 20*, 1457–1480. https://doi.org/10.1111/1541-4337.12709

Rawdkuen, S., D'Amico, S., & Schoenlechner, R. (2022). Physicochemical, functional, and *in vitro* digestibility of protein isolates from Thai and Peru sacha inchi (*Plukenetia volubilis* L.) oil press-Cakes. *Foods, 11*(13), 1869. https://doi.org/10.3390/foods11131869

Rawdkuen, S., Murdayanti, D., Ketnawa, S., & Phongthai, S. (2016). Chemical properties and nutritional factors of pressed-cake from tea and sacha inchi seeds. *Food Bioscience, 15*, 64–71. https://doi.org/10.1016/j.fbio.2016.05.004

Sá, A. G. A., Da Silva, D. C., Pacheco, M. T. B., Moreno, Y. M. F., & Carciofi, B. A. M. (2021). Oilseed by-products as plant-based protein sources: Amino acid profile and digestibility. *Future Foods, 203*, Article 100023. https://doi.org/10.1016/j.fufo.2021.100023

Samad, A., Kumari, S., Hossain, MdJ., Nurul Alam, A. M. M., Kim, S. H., Kim, C. J., et al. (2024). Recent market analysis of plant protein-based meat alternatives and future

prospect. *Journal of Animal & Plant Sciences, 34*(4), 977–987. https://doi.org/10.36899/JAPS.2024.4.0781

Sathe, S. K., Kshirsagar, H. H., & Sharma, G. M. (2012). Solubilization, fractionation, and electrophoretic characterization of Inca peanut (*Plukenetia volubilis* L.) proteins. *Plants Foods for Human Nutrition, 67*, 247–255. https://doi.org/10.1007/s11130-012-0301-5

Sharma, N., Sahil, Madhumita, M., Kumar, Y., & Prabhakar, P. K. (2023). Ultrasonic modulated rice bran protein concentrate: Induced effects on morphological, functional, rheological, and thermal characteristics. *Innovative Food Science and Emerging Technologies, 85*, Article 103332. https://doi.org/10.1016/j.ifset.2023.103332

Shrestha, S., van 't Hag, L., Haritos, V., & Dhital, S. (2023). Comparative study on molecular and higher-order structures of legume seed protein isolates: Lentil, mungbean and yellow pea. *Food Chemistry, 411*, Article 135464. https://doi.org/10.1016/j.foodchem.2023.135464

Suwanangul, S., Sangsawad, P., Alashi, M. A., Aluko, R. E., Tochampa, W., Chittrakorn, S., et al. (2021). Antioxidant activities of sacha inchi (*Plukenetia volubilis* L.) protein isolate and its hydrolysates produced with different proteases. *Maejo International Journal of Science and Technology, 15*(01), 48–60.

Tawalbeh, D., Wan Ahmad, W. A. N., & Sarbon, N. M. (2023). Effect of ultrasound pretreatment on the functional and bioactive properties of legumes protein hydrolysates and peptides: A comprehensive review. *Food Reviews International, 39*(8), 5423–5445. https://doi.org/10.1080/87559129.2022.2069258

Torres-Sánchez, E., Hernández-Ledesma, B., & Gutiérrez, L. F. (2023). Isolation and characterization of protein fractions for valorization of sacha inchi oil press-cake. *Foods, 12*(12), 2401. https://doi.org/10.3390/foods12122401

Wu, W., Jia, J., Wen, C., Yu, C., Zhao, Q., & Hu, J. (2021). Optimization of ultrasound assisted extraction of abalone víscera protein and its effect on the iron-chelating activity. *Ultrasonic Sonochemistry, 77*, Article 105670. https://doi.org/10.1016/j.ultsonch.2021.105670

Zhang, H., Claver, I. P., Zhu, K. X., & Zhou, H. (2011). The effect of ultrasound on the functional properties of wheat gluten. *Molecules, 16*(5), 4231–4240. https://doi.org/10.3390/molecules16054231

Zhao, Y., Wen, C., Feng, Y., Zhang, J., He, Y., Duan, Y., et al. (2021). Effects of ultrasound-assisted extraction on the structural, functional and antioxidant properties of *Dolichos lablab* L. protein. *Process Biochemistry, 101*, 274–284. https://doi.org/10.1016/j.procbio.2020.11.027

Zou, Y., Wang, L., Li, P., Caic, P., Zhang, M., Sun, Z., et al. (2017). Effects of ultrasound assisted extraction on the physiochemical, structural and functional characteristics of duck liver protein isolate. *Process Biochemistry, 52*, 174–182. https://doi.org/10.1016/j.procbio.2016.09.027